PRAMANA
— journal of
physics

Vol. 81, No. 2
August 2013
pp. 261–274

Matter-wave bright solitons in effective bichromatic lattice potentials

GOLAM ALI SEKH
Scientific Computing Laboratory, Institute of Physics Belgrade, Pregrevica 118,
11080 Belgrade, Serbia
E-mail: skgolamali@ipb.ac.rs

MS received 2 November 2012; revised 28 March 2013; accepted 5 April 2013

Abstract. Matter-wave bright solitons in bichromatic lattice potentials are considered and their dynamics for different lattice environments are studied. Bichromatic potentials are created from superpositions of (i) two linear optical lattices and (ii) a linear and a nonlinear optical lattice. Effective potentials are found for the solitons in both bichromatic lattices and a comparative study is done on the dynamics of solitons with respect to the effective potentials. The effects of dispersion on solitons in bichromatic lattices are studied and it is found that the dispersive spreading can be minimized by appropriate combinations of lattice and interaction parameters. Stability of nondispersive matter-wave solitons is checked from phase portrait analysis.

Keywords. Bose–Einstein condensate; optical lattices; inhomogeneous nonlinearity.

PACS Nos 03.75.Lm; 05.45.Yv

1. Introduction

In the past few years, studies on Bose–Einstein condensates (BECs) have gained a tremendous momentum due to the possibility to realize different phenomena of nonlinear optics and condensed-matter physics by controlling different parameters precisely [1]. For example, capability of changing scattering length with the help of Feshbach resonance [2] has allowed to generate the so-called matter-wave solitons [3]. The ability to load BECs in optical lattices has offered possibilities to control the dynamics of mattter-wave solitons [4]. Optical lattice (OL) is a periodic potential produced by two or more counter-propagating laser beams. Depth and geometry of an OL can easily be changed externally. Flexibility of an OL has successfully been used to observe many phenomena such as Josephson effects, squeezed states, Landau–Zener tunnelling and Bloch oscillations, classical and quantum superfluid–Mott insulator transition, Anderson localized waves and gap matter-wave solitons [5].

Formation of solitons and their subsequent evolution are, generally, made in a trap having cigar-shaped geometry [3]. This trapping geometry is obtained by making

DOI: 10.1007/s12043-013-0571-y; ***e*Publication: 1 August 2013**

frequencies of transverse components ($\omega_\perp$) of the confining potential much greater than that of the longitudinal component (ω_x). Additionally, $\omega_\perp$ satisfies the condition $\hbar\omega_\perp \ll \mu$ (μ is the chemical potential) such that the system remains effectively one-dimensional (1D) and contains a phase-coherent sample [4,6]. In cigar-shaped geometry, the BEC is satisfactorily described by means of a mean-field equation, often called Gross–Pitaevskii (GP) equation. The GP equation with an optical lattice potential $V(x)$ in an effective one-dimensional configuration (quasi-one-dimensional (Q1D)) can be written as [4,7]

$$i\frac{\partial\phi}{\partial t} = -\frac{1}{2}\frac{\partial^2\phi}{\partial x^2} + V(x)\phi + \gamma_0|\phi|^2\phi, \tag{1}$$

where $V(x) = V_p\cos(2k_px)$ with V_p and k_p the strength and wavenumber of the OL, and γ_0 is the strength of interatomic interactions. Here, the order parameter $\phi(x,t)$ is normalized to the total number of atoms (N) in the condensate such that $N = \int_{-\infty}^{+\infty} |\phi|^2\, \mathrm{d}x$. In eq. (1), length, time and energy are measured in units of $a_\perp = \sqrt{\hbar/(m\omega_\perp)}$, $\omega_\perp^{-1}$ and $\hbar\omega_\perp$ to make the equation dimensionless. One can experimentally realize the system described in eq. (1) by loading BECs in OLs and then by removing magnetic trap adiabatically. On the other hand, in the real experimental situation ω_x is very small (a few Hz) and its modification over OL is negligible. Equation (1) permits exact bright (dark) soliton solutions when γ_0 is negative (positive) for $V(x) = 0$ [8].

Recently, it has been realized that a BEC can also be loaded in optical potentials resulting from the sequential creations of two lattice structures. Such lattices are often termed as bichromatic lattices. Mathematically, a bichromatic lattice can be described by [9]

$$V_{\mathrm{LL}}(x) = V_p\cos(2k_px) + V_s\cos(2k_sx), \tag{2}$$

where k_s and V_s are respectively the strength and the wavenumber of the additional lattice. Understandably, the first term in (2) is called the primary lattice while the second term is called the secondary lattice. Like primary lattices, the secondary lattice potential in (2) affects only the linear term in (1) and, thus, it is called a secondary linear optical lattice (LOL) and the resulting potential $V_{\mathrm{LL}}(x)$ is termed as a simple bichromatic lattice (SBL).

One can also introduce spatial periodicity in the system by modulating the nonlinear interaction with the help of an optical Feshbach resonance (FR) [10]. Optical FR is similar to magnetic FR. Here a laser beam is tuned close to the resonance of a colliding atom pair with the molecular state in the excited potential (figure 1). In this condition, scattering length can be modified by varying the detuning parameter (Δ) or the intensity I of the laser beam. If we use, for example, a laser beam with intensity $I = I_0\cos^2(k_Nx)$, then the change of scattering length a can be written as

$$a(x) = a_0 + \alpha\frac{I}{(\Delta + I)}.$$

For large detunning ($|\Delta| \gg I$), scattering length can be modified according to

$$a(x) = a_0 + a_1\cos^2(k_Nx).$$

The periodic variation of $a(x)$ can cause same spatially periodic pattern in the interatomic interaction to create the so-called nonlinear optical lattice (NOL).

In the presence of NOL, γ_0 in (1) changes to $\gamma_0 + \gamma_1\cos(2k_Nx)$ [6,12,13], where γ_1 and k_N are respectively the strength and wavenumber of the NOL. As a result, BECs

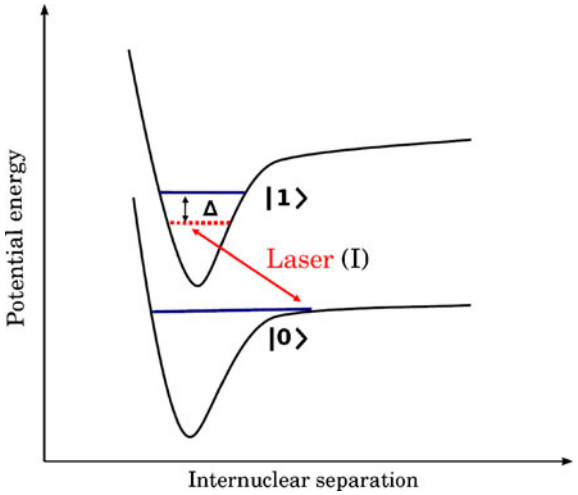

Figure 1. Schematic diagram of an optically-induced Feshbach resonance. A single laser beam of intensity I is used for optically coupling the collisional state $|0\rangle$ to a bound level $|1\rangle$ in the excited molecular potential. Two laser beams, instead of one, can be used to change scattering length more precisely (diagram is not shown) [11].

loaded in a primary optical lattice may also be considered as BECs in mixed bichromatic lattices resulting from the combinations of linear and nonlinear optical lattices. A mixed bichromatic lattice (MBL) can be written as

$$V_{\mathrm{LN}}(x) = V_p \cos(2k_p x) + \gamma_1 \cos(2k_N x)|\phi|^2. \tag{3}$$

Unlike eq. (2), the second term in (3) stands for a secondary NOL. From eqs (2) and (3) we also see that a simple bichromatic lattice potential is state-independent while a mixed bichromatic lattice potential is state-dependent [13].

In general, when a BEC with attractive interatomic interaction is loaded in an OL (primary), its dynamics changes, mainly, due to the new trapping centres introduced by this OL [4]. The sequential presence of another LOL or NOL further affects this dynamics. For example, the spatially periodic variation of interaction between atoms in a BEC loaded in OL can result in delocalized transitions [14] which contrast the behaviour of BECs in OLs with homogeneous atomic interactions. This system can also support gap solitons in the upper half of the forbidden gap even when a_0, the background atomic scattering, is made to vanish. Recently, we have studied that a perturbative NOL makes the localized states in OLs wider while a relatively stronger NOL squeezes these states [6]. An extensive study on the existence, stability and mobility of solitons in BEC with spatially modulated atomic interaction can be found in [15]. Thus, study on the dynamics of solitons under the simultaneous action of two lattices is a subject of considerable current interest.

In the present paper we are trying to do a comparative study on the motion of the matter-wave bright solitons in bichromatic optical lattices which are formed by superpositions of (i) two different linear optical lattices and (ii) a linear and a nonlinear optical lattice. In particular, we emphasize on situations where wavenumbers of the OLs are unequal and

obtain different effective potentials for the solitons. We see that the effective potential for the soliton confined in a primary OL gets modified due to the simultaneous presence of a secondary lattice and the modification depends on relative values of wavenumbers of the OLs. We find that the response of a soliton to the bichromatic lattice potentials is quite interesting. In §2, we reconsider the problem within the framework of variational formulation and obtain expressions for the effective potentials of the solitons embedded in simple and mixed bichromatic lattices. In §3, we study the dynamics of solitons for their different initial locations in the effective potentials. We achieve this goal by direct numerical simulations of the Gross–Pitaevskii equation. In §4, we study variation of soliton's width arising due to dispersion during propagation in the condensates. To that end, we write effective potentials for widths of the matter-wavepackets and also study the nature of stability from phase-portrait diagrams. Finally, in §5, we make some concluding remarks.

2. Variational formulation

The GP equation in (1) is nonintegrable and, thus, it cannot be solved exactly by analytical methods. Therefore, our study is based on an approximate method, namely, the variational method [16]. To proceed with this approach, we restate the initial boundary value problem in (1) as a variational problem

$$\int \mathcal{L}(\phi, \phi^*, \phi_t, \phi_t^*, \phi_x, \phi_x^*)\,\mathrm{d}x\mathrm{d}t = 0. \tag{4}$$

Lagrangian density of (1) obtained from (4) is given by

$$\begin{aligned}\mathcal{L} = {} & \frac{i}{2}(\phi\phi_t^* - \phi^*\phi_t) + \frac{1}{2}\phi_x\phi_x^* + V_p\cos(2k_px)\phi\phi^* \\ & + V_j(x)\phi\phi^* + \frac{1}{2}\gamma_0\phi^2\phi^{*2}, \quad j = 1, 2,\end{aligned} \tag{5}$$

where $V_1(x) = V_s\cos(2k_sx)$ and $V_2(x) = \frac{1}{2}\gamma_1\cos(2k_Nx)|\phi|^2$ stand for secondary lattice potentials which contribute to create simple and mixed bichromatic optical lattices respectively. In the variational formulation, one of the main tasks is to find a suitable trial solution for the system. We know that in the absence of OLs, the solution of (1) for self-focussing nonlinear interactions is a sech function [17] with constant parameters. To incorporate the effects of optical lattices, we postulate that these parameters become time-dependent. Thus, we write the trial solution as [18,19]

$$\phi(x,t) = A(t)\mathrm{sech}\left[\frac{(x - x_0(t))}{a(t)}\right]\mathrm{e}^{[i\dot{x}_0(x-x_0(t))+i\beta(t)(x-x_0(t))^2+i\Phi(t)]}, \tag{6}$$

where $A(t)$ is the real amplitude, $a(t)$ is the width, $x_0(t)$ stands for the position of the centre of mass, $\Phi(t)$ is the phase and $\beta(t)$ is the frequency chirp of the matter-wavepacket. Clearly, $\dot{x}_0 = \mathrm{d}x_0/\mathrm{d}t$. Inserting (6) in (5) and integrating the resulting $\mathcal{L}$ over x from $-\infty$ to $+\infty$, we get the average Lagrangian density

$$\begin{aligned}\langle\mathcal{L}\rangle = {} & \frac{A^2}{3a} + \frac{2}{3}\gamma_0 aA^4 + 2\pi V_p a^2A^2\frac{\cos(2k_px_0)}{\sinh(\pi ak_p)}k_p + \frac{1}{3}\pi^2a^3A^2\beta^2 - aA^2\dot{x}_0^2 \\ & + \frac{1}{6}\pi^2a^3A^2\dot{\beta} + 2aA^2\Phi' + \langle\mathcal{L}_S^{(j)}\rangle, \qquad j = 1, 2,\end{aligned} \tag{7}$$

where

$$\langle \mathcal{L}_S^{(1)} \rangle = 2\pi V_s a^2 A^2 \frac{\cos(2k_s x_0)}{\sinh(\pi a k_s)} k_s$$

and

$$\langle \mathcal{L}_S^{(2)} \rangle = \frac{2}{3}\pi \gamma_1 a^2 A^4 \frac{\cos(2k_N x_0)}{\sinh(\pi a k_N)} k_N (1 + a^2 k_N^2). \tag{8}$$

Clearly, $\langle \mathcal{L}_S^{(1)} \rangle$ and $\langle \mathcal{L}_S^{(2)} \rangle$ in (8) stand for the average Lagrangian densities resulting from the secondary linear and nonlinear optical lattices respectively. We now apply Ritz optimization ($(\delta \langle \mathcal{L} \rangle / \delta \sigma) = 0$ with $\sigma (= A, a, x_0, \beta$ and $\Phi)$) to (7) with a view to get equations for the variational parameters. Appropriate combinations of these equations give ordinary differential equations for different physical quantities of bright matter-wavepackets in bichromatic optical lattices:

$$\frac{\mathrm{d}}{\mathrm{d}t}[2aA^2] = 0, \tag{9a}$$

$$-2\pi V_p a k_p^2 \frac{\sin(2k_p x_0)}{\sinh(\pi a k_p)} - 2\pi V_s a k_L'^2 \frac{\sin(2k_s x_0)}{\sinh(\pi a k_s)} + \ddot{x}_0 = 0 \tag{9b}$$

and

$$\frac{4}{\pi^2 a^3} + \frac{2N\gamma_0}{\pi^2 a^2} - \frac{12 V_p a k_p}{\pi} \frac{\cos(2k_p x_0)}{\sinh(\pi a k_p)} [1 - \pi a k_p \coth(\pi a k_p)] - \frac{12 V_p a k_p}{\pi} \frac{\cos(2k_p x_0)}{\sinh(\pi a k_p)} [1 - \pi a k_p \coth(\pi a k_p)] - \ddot{a}_0 = 0. \tag{9c}$$

In conjunction with the normalization condition $\left(\int_{-\infty}^{+\infty} |\phi|^2 \mathrm{d}x = N\right)$, eq. (9a) gives that the number of atom in the system is conserved. For this conservative system, eq. (9b) describes the evolution of the centre of the soliton. Variations of soliton's widths can be determined from eq. (9c) also.

In the above, we present equations for parameters of a matter-wavepacket in simple bichromatic lattices (SBLs). Similar equations for solitons in mixed bichromatic lattices (MBLs) are given by

$$-2\pi V_p a k_p^2 \frac{\sin(2k_p x_0)}{\sinh(\pi a k_p)} - \frac{1}{3} N \pi \gamma_1 \frac{\sin(2k_N x_0)}{\sinh(\pi a k_N)} k_N^2 (1 + a^2 k_N^2) + \ddot{x}_0 = 0, \tag{10a}$$

and

$$\frac{4}{\pi^2 a^3} + \frac{2N\gamma_0}{\pi^2 a^2} - \frac{12 V_p a k_p}{\pi} \frac{\cos(2k_p x_0)}{\sinh(\pi a k_p)} [1 - \pi a k_p \coth(\pi a k_p)] + \frac{2N\gamma_1}{\pi} a k_N^2 \frac{\cos(2k_N x_0)}{\sinh(\pi a k_N)} [\pi \coth(\pi a k_N) - 2a k_N + \pi a^2 k_N^2 \coth(\pi a k_N)] - \ddot{a}_0 = 0. \tag{10b}$$

Note that, for MBL, we have an equation similar to eq. (9a). This implies that the BEC in MBLs is also a conservative system. In the next sections, we shall judiciously use eqs (9) and (10) to extract information on the dynamics and stability of matter-wavepackets in bichromatic lattices.

3. Matter-wave with different lattice environments

In analogy with the propagation of optical pulses in transparent medium, the matter-wave in BEC may acquire a chirp due to the effects of nonlinearities during its motion. This chirp causes the instantaneous frequency of the wavepacket to change with time. If the instantaneous frequency rises (decreases) then we have an up-chirp (down-chirp) [20]. The main effect of the chirp is that it minimizes propagation durations of wavepackets in nonlinear media. In the present case, the appearance of chirp introduces a change in the width [$\partial\langle\mathcal{L}\rangle/\partial\beta = 0,\ \mathrm{d}a/\mathrm{d}t = 2\beta a$] that may induce instability and may be responsible for the short duration of propagation. In the context of nonlinear optics, it may be noted that the chirp of a pulse can be removed by propagating it through optical components with suitable dispersion. In view of this, we consider, in this section, the dynamics of wavepackets neglecting instantaneous frequency change over it.

The dynamics of matter-wave solitons in bichromatic lattice potentials, as noted above, can be described by the equations of $x_0(t)$ in (9b) and (10a). These are second-order ordinary differential equations that can be used to extract effective potential for the centre of the wavepacket by rewriting them in the form of Newtonian equations

$$\ddot{x}_0 = -\frac{\mathrm{d}V_{\mathrm{eff}}}{\mathrm{d}x_0}, \tag{11}$$

where V_{eff} is the effective potential. For the simple bichromatic lattice (SBL) V_{eff} is given by

$$V_{\mathrm{SBL}}(x_0) = \frac{\pi V_p k_p a}{\sinh(\pi a k_p)}\cos(2k_p x_0) + \frac{\pi V_s k_s a}{\sinh(\pi a k_s)}\cos(2k_s x_0). \tag{12a}$$

Similarly, for the mixed bichromatic lattice (MBL) V_{eff} is given by

$$\begin{aligned} V_{\mathrm{MBL}}(x_0) \;=\; & \frac{\pi V_p k_p a}{\sinh(\pi a k_p)}\cos(2k_p x_0) \\ & + \frac{\pi}{6}\frac{N\gamma_1 k_N(1+k_N^2 a^2)}{\sinh(\pi a k_N)}\cos(2k_N x_0). \end{aligned} \tag{12b}$$

The Newtonian equation in (12) describes a particle moving in a potential V_{eff}. Velocity of this particle obtained from (12) is given by

$$\dot{x}_0 = \pm\sqrt{C_0 - 2V_{\mathrm{eff}}}, \tag{13}$$

where C_0 is the value of V_{eff} at $t = 0$, i.e., at $x_0 = x_0(0)$. From (13) it is clear that for both SBL and MBL, the velocity of the soliton changes with different values of V_{eff}. Initial velocity of motion is determined by both lattice and soliton parameters, and also by $x_0(0)$. On the other hand, from (12a) and (12b), we see that V_{eff} arises from superpositions

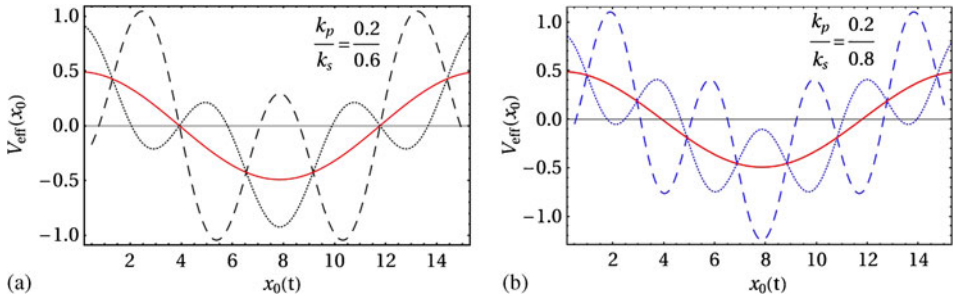

Figure 2. Effective potential V_{eff} as a function of x_0 for $N = 5, \gamma_0 = -1, a = 0.5$, $V_p = 0.5, V_s = 0.5, \gamma_1 = -0.5$. **(a)** shows V_{eff} for $k_p/k_s = 0.2/0.6$ while **(b)** shows V_{eff} for $k_p/k_s = 0.2/0.8$. Dotted and dashed curves in both panels represent $V_{\text{SBL}}(x_0)$ and $V_{\text{MBL}}(x_0)$.

of two periodic potentials, namely, primary and secondary optical lattices. For bright solitons ($\gamma_1 = -|\gamma_1|$) embedding in the SBL, these two lattices are in-phase (eq. (12a)) while in the MBL they are out of phase (eq. (12b)). In addition, magnitudes of secondary lattice potentials in SBL and MBL are different since their dependence on a are different due to their different origins. Therefore, it is interesting to see how the effective potentials for solitons in simple and mixed bichromatic lattices are modified by varying the lattice and soliton parameters.

In view of the above, we plot in figure 2, V_{eff} as a function of x_0 for different spatially incommensurable lattice periods. Figure 2a shows V_{eff} for $k_p/k_s = 0.2/0.6$ while figure 2b shows V_{eff} for $k_p/k_s = 0.2/0.8$. From the curves in these figures we see that the superposition of a secondary lattice with the primary lattice creates new intensity distribution patterns. As a result, some new local minima appear inside the minima of the primary lattice. Depth and position of these minima are different for different bichromatic lattices due to their unequal dependence on different parameters. For example, strength of the secondary lattice in MBL (eq. (12b)) is proportional to N while it does not explicitly depend on N in SBL (eq. (12a)). In both cases, the effective potential varies with the change of lattice incommensurability but these changes are not the same in MBL and SBL even when other parameters are the same. Various incommensurabilities are responsible for various locations of minima which may support stable minicondensates (figures 2a and 2b).

In order to examine the ability of linear and nonlinear secondary lattices in altering the dynamics of solitons by introducing extrema, we consider time evolution of wavepackets in non-dispersive condensate media. In particular, we consider different initial locations x_0 ($=x_0(0)$) with respect to the effective potential V_{eff} for $k_p/k_s = 0.2/0.6$ (figure 2a) in SBL (dotted curve). We take three x_0 values, namely, $x_0 = 8$, 10 and 13 to account for three different initial environments of solitons in the lattice. Clearly, the initial environments of solitons embedded in SBLs and MBLs are not the same even for the same x_0 values. For example, the point $x_0 = 8$ corresponds to a minimum (maximum) of SBLs (MBLs) while $x_0 = 10$ and $x_0 = 13$ respectively stand for maximum (minimum) and second minimum (maximum) for SBLs (MBLs). To that end, we solve (1) numerically using the Method of Lines (MOL) algorithm [21] with the help of *Mathematica*

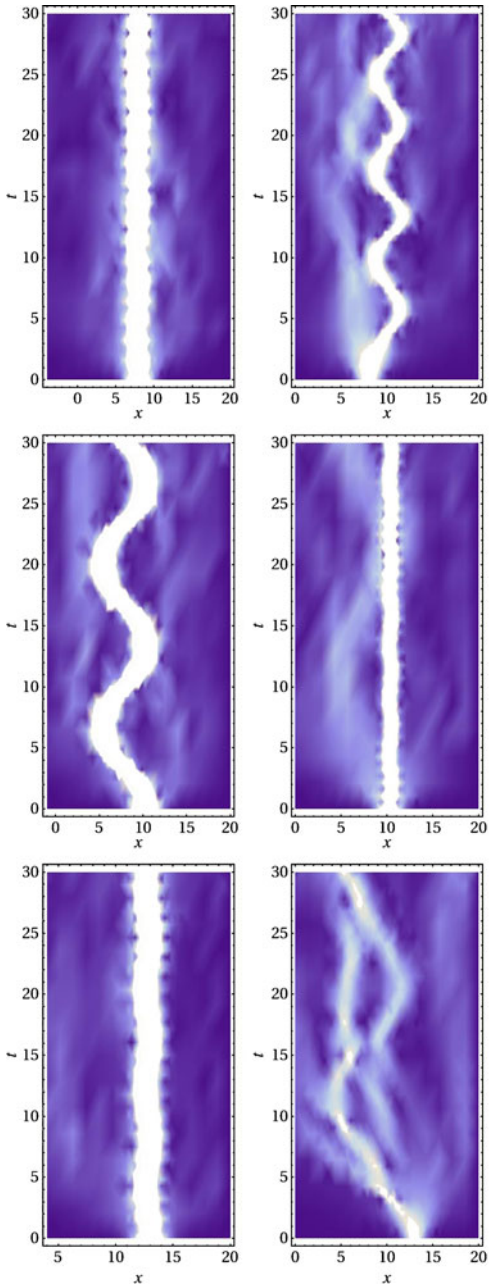

Figure 3. Evolution of density profiles in bichromatic lattices with wavenumber ratio $k_p/k_s = k_p/k_N = 0.2/0.6$, $V_s = 0.5$, $V_p = 0.5$, $\gamma_0 = -1.0$, $\gamma_1 = -0.5$, $N = 5$ and $a = 0.5$. Three pairs of density plots are displayed for different initial environments, namely, top pair for $x_0 = 8$, middle and bottom pairs for $x_0 = 10.25$ and 13. In each pair, left panel gives density plot of the wavepackets in SBL while right panel gives density plots of the wavespackets in MBL.

[22] for $\phi(x,0) = A\,\mathrm{sech}[(x-x_0)/a]$ and $\phi(-25,t) = \phi(25,t)$ as initial and boundary conditions.

The evolution of soliton's density profiles in simple and mixed bichromatic lattices are shown pairwise in figure 3. In each pair (top, middle and bottom), left panel gives density of solitons in SBL and right panel gives the same in MBL. In the top pair, soliton in SBL at $x_0 = 8$ (left panel) does not move with time. However, for the same initial position, the soliton in MBL starts to oscillate about the nearest minimum in the effective position (right panel). This can be explained in the following way. At $x_0 = 8$ in SBL, no energy transfer takes place from the lattice to the soliton. As a result, the soliton does not gain any energy to move or to suffer from instability. In MBL, the soliton at $x_0 = 8$ acquires some energy from the lattice resulting in an increase of its kinetic energy (KE). The excess KE causes the soliton to move towards a minimum energy location and to oscillate about that minimum. Here the gained energy is still too low to induce instability.

For $x_0 = 10.25$ (middle pair), the new lattice environment leads the soliton in SBL to a nearest stable configuration position (minimum energy) by transferring some energy to it. Here also, the additional energy manifests as periodic motion (left panel). The soliton at $x_0 = 10.25$ in MBL, however, gets the lowest energy position and does not move with time (right panel).

The solition in SBL at $x_0 = 13$ (bottom pair) again gets a minimum energy location and, therefore, no energy transfer takes place from the lattice to the wavepackets. As a result, the soliton neither propagates nor gets excitation that induces instability (left panel). The local maxima at $x_0 = 13$ in MBL, on the other hand, transfers sufficient energy to the soliton. The excess energy here is enough to induce instability by creating imbalance between nonlinearity and lattice energy. The induced instability leads the soliton to decay during propagation (right panel).

4. Matter-wavepackets with dispersion

In this section, we consider the effects of dispersion which cause decay of matter-wavepacket with time. In the present formulation, this dispersion is introduced by frequency chirp which makes width of the wavepacket time-dependent. In view of this, we ignore motion of the centre of mass and concentrate on the change of width with time. Equations for widths of the solitons in simple and mixed bichromatic lattices are given by

$$\frac{4}{\pi^2 a^3} + \frac{2N\gamma_0}{\pi^2 a^2} - \frac{12V_p a k_p}{\pi \sinh(\pi a k_p)}[1 - \pi a k_p \coth(\pi a k_p)] - \frac{12V_s a k_s}{\pi \sinh(\pi a k_s)}[1 - \pi a k_s \coth(\pi a k_s)] - \ddot{a}_0 = 0 \tag{14}$$

and

$$\frac{4}{\pi^2 a^3} + \frac{2N\gamma_0}{\pi^2 a^2} - \frac{12V_p a k_p}{\pi \sinh(\pi a k_p)}[1 - \pi a k_p \coth(\pi a k_p)] + \frac{2N\gamma_1 a k_N^2}{\pi \sinh(\pi a k_N)}[\pi \coth(\pi a k_N) - 2a k_N + \pi a^2 k_N^2 \coth(\pi a k_N)] - \ddot{a}_0 = 0. \tag{15}$$

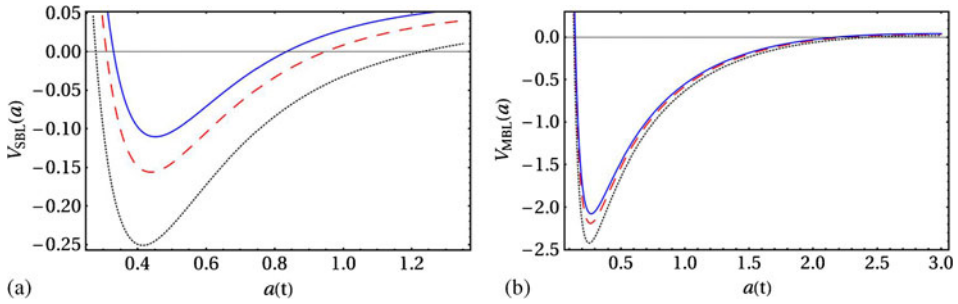

Figure 4. Effective potential V_{eff} as function of a for $V_p = 0.5$, $V_s = 0.5$, $\gamma_1 = -0.5$, $\gamma_0 = -1.0$ and $k_p/k_s = 0.2/0.6$. **(a)** gives V_{SBL} while **(b)** gives V_{MBL}. The solid, dotted and dashed curves stand for effective potentials for $N = 4.8$, 5.0 and 5.2.

[Equations (14) and (15) are written respectively from (9c) and (10b) with $x_0 = 0$]. Effective potentials for the widths can be written as

$$V_{\text{SBL}}(a) = \frac{2}{\pi^2 a^2} + \frac{2N\gamma_0}{\pi^2 a} + \frac{12V_p k_p}{\pi}\frac{a}{\sinh(\pi k_p a)} + \frac{12k'V_s}{\pi}\frac{a}{\sinh(\pi k' a)} \tag{16}$$

$$V_{\text{MBL}}(a) = \frac{2}{\pi^2 a^2} + \frac{2N\gamma_0}{\pi^2 a} + \frac{12V_p k_p}{\pi}\frac{a}{\sinh(\pi k_p a)} + \frac{2N\gamma_1 k_N}{\pi \sinh(\pi a k_N)}(1+a^2k_N^2). \tag{17}$$

The effective potentials for widths in eqs (16) and (17) contain two extra terms compared to V_{eff} for x_0. First term can be interpreted as a dispersive term while the second term resulted from nonlinearity which opposes effects of the first term when $\gamma_0 < 0$. Note that the lattice potential terms (third and fourth terms) may either help or oppose first and second terms depending on their signs. With a view to find exact contribution of these terms to support non-dispersive matter-wave, we plot V_{SBL} in figure 4a and V_{MBL} in figure 4b with a for different negative values of γ_0. We notice that for $\gamma_0 = 0$, effective potential decreases monotonically (not shown in figure 4). This implies that optical lattice alone could not stop the expansion of $a(t)$. For appropriate values of $-\gamma_0$ and/or N, the nonlinear term interplays with OLs in such a way that their resulting potential can balance the dispersive term to stop spreading bright solitons.

From figures 4a and 4b, we see that the potential becomes zero for $a = a_l$ and a_r. Between a_l and a_r there is a minimum at $a = a_m$. This implies that spreading of matter-wave starts at a_l and stops at a_r. After reaching a_r it starts to compress and continues up to a_l through a_m. In this way, width of the wavepacket oscillates between a_l ad a_r with time during propagation. Clearly, the variation of $a(t)$ with time in MBL is larger than that in SBL. We calculate frequency of oscillation (ν) of width linearizing eqs (14)

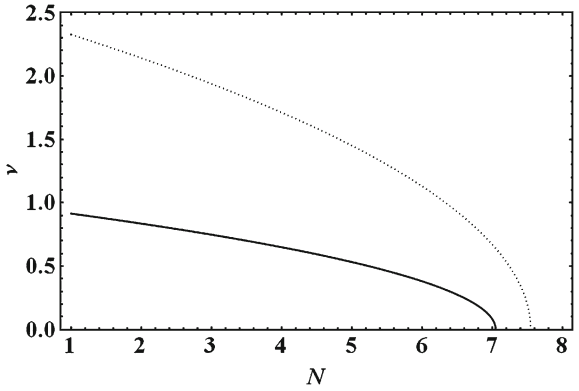

Figure 5. Frequency as a function of N for $V_p = 0.5$, $V_s = 0.5$, $\gamma_1 = -0.5$, $\gamma_0 = -1.0$ and $k_p/k_s = 0.2/0.6$. The solid and dotted curves give results for SBL and MBL around their stable equilibrium points a_0, namely, $a_0 = 0.425$ and $a_0 = 0.365$.

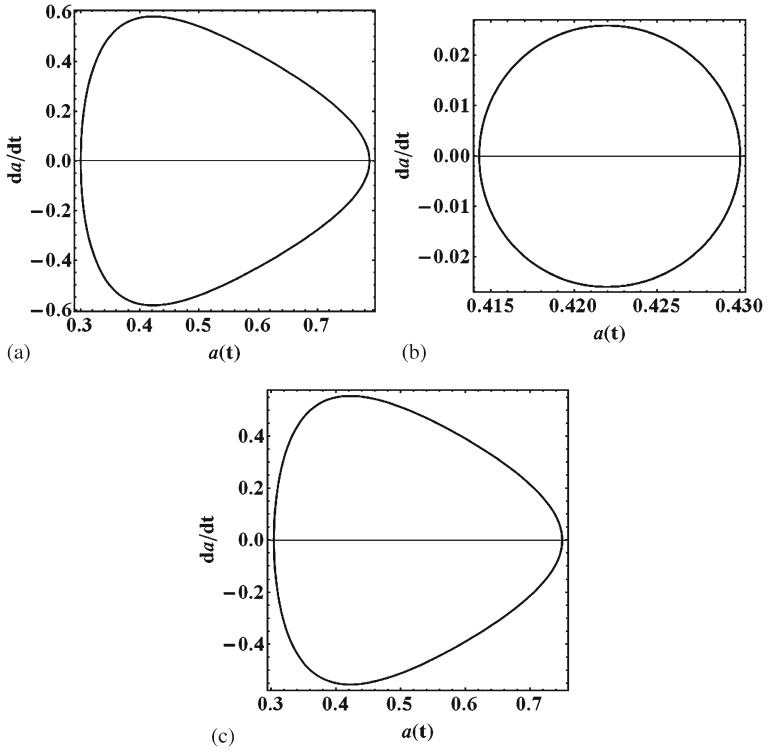

Figure 6. Phase portrait of soliton's width in BEC embedded in simple bichromatic lattices (SBL) for $N = 5$, $V_p = 0.5$, $V_s = 0.5$, $\gamma_1 = -0.5$, $\gamma_0 = -1.0$. (**a**) $\dot{a}(0) = 0, a(0) = 0.3$, (**b**) $\dot{a}(0) = 0, a(0) = 0.43$ and (**c**) $\dot{a}(0) = 0, a(0) = 0.75$.

and (15) about the minima of V_{SBL} and V_{MBL} respectively. Frequency (ν) vs. N curve in figure 5 shows that the frequency ν decreases with the increase in N (or γ_0). This implies that, for larger N, effective interatomic interaction becomes strong enough to hold the atoms tightly and to oppose change of the width of soliton with time. Note that frequency of fluctuation of soliton's width in MBL (dotted curve) is always greater than that in SBL (solid curve) because of the state-dependent nature of the NOL. However, the fluctuation of width in both bichromatic lattices reduces to zero at a particular value of N, say, N_m. Figure 5 indicates that the value of N_m in MBL is greater than that in SBL.

Dynamical characteristics of the system can also be checked from the phase portraits. It is easy to construct qualitative phase portrait from V_{SBL} or V_{MBL} for the nonlinear conservative systems given in eqs (16) and (17) [23]. Phase portraits of soliton's widths for SBLs and MBLs are displayed respectively in figures 6 and 7. At the minima of both V_{SBL} and V_{MBL} we get centre-type equilibrium states (b). In the neighbourhood of the centre (on either side of the minimum) these curves have ellipse-like shapes but they are deformed when moving away from the centre. We see that, for both SBL and MBL, phase diagrams are the same. The only difference is that a stable centre occurs in MBL for relatively smaller value of a [6].

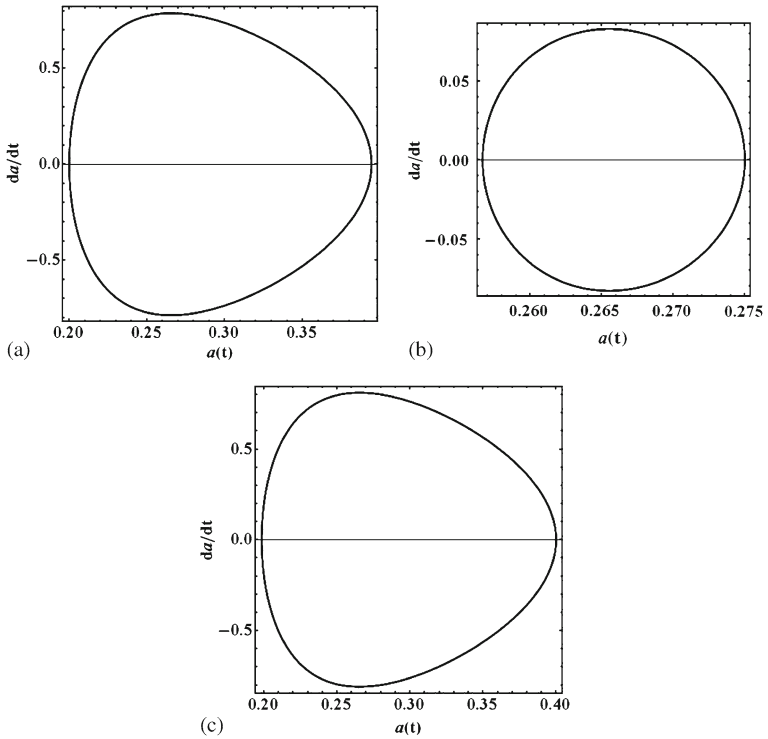

Figure 7. Phase portrait of soliton's width in BEC embedded in mixed bichromatic lattices (MBLs) for $N = 5$, $V_p = 0.5$, $V_s = 0.5$, $\gamma_1 = -0.5$, $\gamma_0 = -1.0$. (**a**) $\dot{a}(0) = 0, a(0) = 0.242$, (**b**) $\dot{a}(0) = 0, a(0) = 0.265$ and (**c**) $\dot{a}(0) = 0, a(0) = 0.3$.

5. Conclusion

We have studied the dynamics of matter-wave bright solitons in simple (SBL) and mixed bichromatic (MBL) optical lattices within the framework of variational approach. Considering bichromatic lattice as superpositions of two lattices of spatially incommensurate periodicities, we have constructed effective potentials for the centre of solitons embedded in those lattices. It is seen that dynamics of the matter-wave depends sensitively on initial environments in both bichromatic lattices. However, for the same initial environments in the SBL and MBL, solitons execute different dynamics because of their different origins.

We have investigated the dispersive nature of matter-waves by constructing effective potentials for widths. It is noted that the size of a wavepacket changes during evolution keeping the number of atoms (N) constant. The frequency of changing size varies with N and/or with strength of atomic interactions. This change of size can be removed/minimized by suitably choosing lattice and soliton parameters. We have found that the fluctuation in size of a wavepacket in MBL is always greater than that of a wavepacket in SBL. We have also found that, around stable equilibrium, the number of atoms required to propagate a fixed size wavepacket in MBL is greater than that needed in SBL even when other parameters are identical.

We have envisaged a brief dynamical systems theory analysis to examine the nature of stability with the help of effective potentials. It is seen that, at the minima of the potential, the system has a centre. This analysis also leads us to conclude that a stable soliton supported by mixed bichromatic lattices is narrower than that supported by simple bichromatic lattices.

Acknowledgements

The author would like to thank Antun Balaž for providing research fund and other facilities during this work. The author would also like to thank Afrin Sultana for carefully reading the manuscript.

References

[1] F Dalfavo, S Giorgini, L P Pitaevskii and S Stringari, *Rev. Mod. Phys.* **71**, 463 (1999)
Anthony J Leggett, *Rev. Mod. Phys.* **73**, 307 (2001)
I Bloch, J Dalibard and W Zwerger, *Rev. Mod. Phys.* **80**, 885 (2008)
S Giorgini, L P Pitaevskii and S Stringari, *Rev. Mod. Phys.* **80**, 1215 (2008)

[2] H Feshbach, *Ann. Phys. (N.Y.)* **5**, 375 (1958)
S Inouye, M R Andrews, J Stenger, H-J Miesner, D M Stamper-Kurn and W Ketterle, *Nature* **392**, 151 (1998)

[3] Kevin E Strecker, Guthrie B Partridge, Andrew G Truscott and Randall G Hulet, *Nature* **417**, 150 (2002)
L Khaykovich, F Schreck, G Ferrari, T Bourdel, J Cubizolles, L D Carr, Y Castin and C Salomon, *Science* **296**, 1290 (2002)

[4] O Morsch and M Oberthaler, *Rev. Mod. Phys.* **78**, 179 (2006)

[5] F S Cataliotti, S Burger, C Fort, P Maddaloni, F Minardi, A Trombettoni, A Smerzi and M Inguscio, *Science* **293**, 843 (2001)

L Fallani, F S Cataliotti, J Catani, C Fort, M Modugno, M Zawada and M Inguscio, *Phys. Rev. Lett.* **91**, 240405 (2003)
M Cristiani, O Morsch, J H Müller, D Ciampini and E Arimondo, *Phys. Rev. A* **65**, 063612 (2002)
B P Anderson and M A Kasevich, *Science* **282**, 1686 (1998)
O Morsch, J H Müller, M Cristiani, D Ciampini and E Arimondo, *Phys. Rev. Lett.* **87**, 140402 (2001)
M Greiner, O Mandel, T Esslinger, T W Hänsch and I Bloch, *Nature* **415**, 39 (2002)
G Roati, C D'Errico, L Fallani, M Fattori, C Fort, M Zaccanti, G Modugno, M Modugno and M Inguscio, *Nature* **453**, 895 (2008)
B Eiermann, Th Anker, M Albiez, M Taglieber, P Treutlein, K-P Marzlin and M K Oberthaler, *Phys. Rev. Lett.* **92**, 230401 (2004)
D Mandelik, R Morandotti, J S Aitchison and Y Silberberg, *Phys. Rev. Lett.* **92**, 093904 (2004)

[6] S Golam Ali, B Talukdar and S K Roy, *Eur. Phys. J. D* **59**, 269 (2010)

[7] V A Brazhnyi and V V Konotop, *Mod. Phys. Lett. B* **18**, 627 (2004)
P G Kevrekidis and D J Frantzeskakis, *Mod. Phys. Lett. B* **18**, 173 (2004)

[8] D L Mills, *Nonlinear optics* (Springer-Verlag, 1998), ISBN-13:978-3540641827

[9] S Peil, J V Porto, B L Tolra, J M Obrecht, B E King, M Subbotin, Rolston and W D Phillips, *Phys. Rev. A* **67**, 051603(R) (2003)
Mason A Porter, P G Kevrekidis, R Carretero-Gonzalez and D J Frantzeskakis, *Phys. Lett. A* **352**, 210 (2006)

[10] P O Fedichev, Yu Kagan, G V Shlyapnikov and J T M Walraven, *Phys. Rev. Lett.* **77**, 2913 (1996)
M Theis, G Thalhammer, K Winkler, M Hellwig, G Ruff, R Grimm and J H Denschlag, *Phys. Rev. Lett.* **93**, 123001 (2004)

[11] Gregor Thalhammer, Matthias Theis, Klaus Winkler, Rudolf Grimm and Johannes Hecker Denschlag, *Phys. Rev. A* **71**, 033403 (2005)

[12] H Sakaguchi and B A Malomed, *Phys. Rev. E* **72**, 046610 (2005)

[13] F Kh Abdullaev, A Gammal, M Salerno and L Tomio, *Phys. Rev. A* **367**, 149 (2008)

[14] Yu V Bludov, V A Brazhnyi and V V Konotop, *Phys. Rev. A* **76**, 023603 (2007)

[15] H Sakaguchi and B A Malomed, *Phys. Rev. A* **81**, 013624 (2010)
Yaroslav V Kartashov, Boris A Malomed and Lluis Torner, *Rev. Mod. Phys.* **83**, 247 (2011)

[16] D Anderson, *Phys. Rev. A* **27**, 3135 (1983)

[17] V E Zakharov and A B Shabat, *Sov. Phys. JETP* **34**, 62 (1972)

[18] Y Cheng, R Gong and H Li, *Opt. Express* **14**, 3594 (2006)

[19] Sk Golam Ali and B Talukdar, *Ann. Phys. (N.Y.)* **324**, 1194 (2009)

[20] R Paschotta, Field guide to optical fiber technology (SPIE Press Book, 2010), ISBN:9780819480903

[21] W E Schiesser, *The numerical method of lines: Integration of partial differential equations* (Academic Press, San Diego, 1991)

[22] S Wolfram, *Mathematica, A system for doing mathematics by computer*, Version 6.0 (Wolfram Research Inc, New York, 2007)

[23] Vadim S Anishchenko *et al*., *Nonlinear dynamics of chaotic and stochastic systems: Tutorial and modern development*, Springer Series in Synergetics, ISBN:978-3-540-38168-6